Geophysical Research Letters

RESEARCH LETTER
10.1029/2019GL082159

Secular Drift of the Auroral Ovals: How Fast Do They Actually Move?

N. A. Tsyganenko[1]

[1]Institute and Department of Physics, Saint-Petersburg State University, Saint-Petersburg, Russia

Key Points:
- From 1965 to 2020 the Northern auroral oval drifted by 4-5 degrees of latitude, comparable with centered, eccentric, and corrected pole shifts
- The 15-degree jump of the Northern dip pole over the same period is irrelevant to the auroral oval shift and is a largely geometric effect
- Southern oval shift over the same period, its shape, and pole behavior are drastically asymmetric to those in the Northern Hemisphere

Correspondence to:
N. A. Tsyganenko,
n.tsyganenko@spbu.ru

Citation:
Tsyganenko, N. A. (2019). Secular drift of the auroral ovals: How fast do they actually move? *Geophysical Research Letters*, *46*, 3017–3023. https://doi.org/10.1029/2019GL082159

Received 22 JAN 2019
Accepted 27 FEB 2019
Accepted article online 4 MAR 2019
Published online 18 MAR 2019

Abstract A surprisingly fast secular drift of the Northern geomagnetic dip pole during the last two decades has attracted much interest lately, in particular, evoking speculations about a possibility of a sweeping relocation of the auroral oval. This letter presents first results of a model investigation of this issue, based on an empirical representation of the distant magnetosphere combined with a series of internal geomagnetic field models for 12 epochs, covering the interval from 1965 to 2020. The secular drift of the northern auroral oval was found to result in its net displacement over the 55-year period, commensurate with the concurrent shifts of the centered, eccentric, and corrected geomagnetic poles, all of them much smaller than the enormous spurt of the northern dip pole. In the Southern Hemisphere, the shift of the auroral oval and of the poles over the same period is much weaker, revealing a remarkable interhemispheric asymmetry.

Plain Language Summary The auroral displays associated with space storms occur within two band-like regions, encircling north and south polar caps and called auroral ovals. Aside from highly dynamical reconfigurations of the ovals during space weather events, there exists a much slower and steady shift of their position, associated with a gradual change of the geomagnetic field, termed secular variations and closely related to slow relocation of the geomagnetic poles over the Earth's surface. A remarkable phenomenon observed during the last few decades is an unusually fast shift of the geomagnetic dip pole (a point with strictly vertical field direction) from North Canada toward East Siberia. A natural question is then: how large is the secular shift of the auroral ovals in comparison with the fast relocation of the dip pole? In this work, the problem is addressed from the viewpoint of a magnetospheric model based on spacecraft data. It is shown that the secular shift of the auroral oval between 1965 and 2020 is about the same as that of the geomagnetic dipole axis, which is much slower than the fastly racing dip pole. In the Southern Hemisphere, the oval shifts are much smaller than in the Northern Hemisphere.

1. Introduction

Recent decades have seen a remarkable acceleration of the secular drift of the geomagnetic dip pole in the Northern Hemisphere from Arctic Canada toward the coast of Eastern Siberia (e.g., Mandea & Dormy, 2003). As of present, the North dip pole is crossing the border between the western and eastern hemispheres, in only ~400 km from the north geographic pole. In view of such dramatic displacement, a natural question arises: how large and fast is the associated secular shift of the auroral ovals? In the existing literature, a similar problem was addressed by Oguti (1993) who assessed the expected long-term changes of the oval shape/size in both hemispheres between the end of the twentieth century and up to 1000 years into the future. That study did not involve any magnetosphere model but relied solely on an internal field representation by spherical harmonics and its forward extrapolation in time. The auroral oval shapes were defined as loci of footpoints of magnetic field lines, whose apex field magnitudes fell within an a priori prescribed interval, calculated from a purely dipolar model.

This letter presents first results based on a different approach, in which the auroral oval is explicitly defined using an empirical model of the magnetosphere in combination with a series of standard internal magnetic field models. Also, instead of analyzing long-term future trends, this study focuses on the recent 55-year interval covering the 1965–2020 epochs. Note from the outset that the present work addresses exclusively the impact of secular variations of the main field, but leaves aside the effect of changing interplanetary conditions. To that end, only a single variant of the external field model is employed, corresponding to an average slightly disturbed state of the magnetosphere. Furthermore, to abstract from seasonal and diurnal effects of

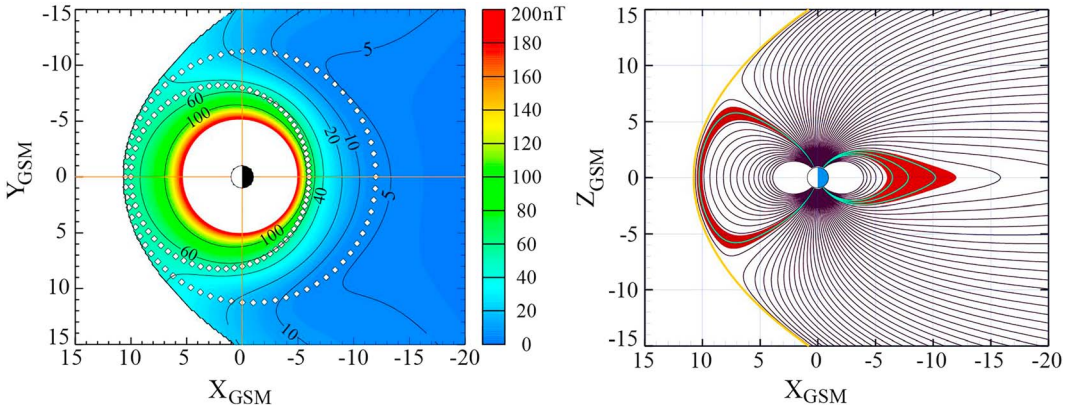

Figure 1. Illustrating the auroral oval definition, based on the TA15 magnetosphere model. (left) Quasi-circular contours confining the oval domain in the geocentric solar magnetospheric equatorial plane (white dots), shown against the color-coded distribution of the total field intensity. The color scale saturates in the inner magnetosphere at $R < 5$ (white circle). (right) Model field lines in the noon–midnight meridional plane; the auroral oval domain is highlighted with dark red.

the geodipole wobbling, only north-south symmetric configurations are analyzed, with the dipole tilt angle $\Psi = 0$. It is demonstrated below that the secular shift of the northern auroral oval between 1965 and 2020 is comparable in magnitude and occurred roughly in the same direction as the concurrent displacement of the magnetic poles, defined on the basis of centered, eccentric, and corrected dipole models. All these shifts are shown to be much smaller (by a factor of 4–5) than the dramatic spurt of the northern dip pole.

In the Southern Hemisphere the oval's shift is much weaker than in the Northern Hemisphere, and its shape is much closer to circular. The problem of the north-south interhemispheric asymmetry of high-latitude/low-altitude magnetic fields has many interesting implications, in particular, with respect to the ionospheric response to the solar wind driving. A comprehensive analysis of the north-south asymmetries of the high-latitude geomagnetic field can be found in a recent review by Laundal et al. (2017), focused on the pole locations and magnetic conjugacy aspects. The present paper addresses a closely related matter concerning the N-S asymmetry of the auroral ovals, objects of major importance in space weather studies.

2. Details of the Method and Results

To represent the external part of the magnetospheric magnetic field, we used a recent TA15 model (Tsyganenko & Andreeva, 2015), parameterized by the solar wind dynamic pressure P_d, dipole tilt Ψ, transverse part $\mathbf{B}_\perp$ of the interplanetary magnetic field (IMF), and the N index by Newell et al. (2007) quantifying the intake rate of the interplanetary magnetic flux and defined as a function of the solar wind speed V, $B_\perp$, and the IMF clock angle θ as $N = 10^{-4}V^{4/3}B^{2/3}\sin^{8/3}(\theta/2)$. In all calculations, a weakly disturbed magnetosphere was assumed with $P_d = 1.7$ nPa, IMF $B_y = 0$, $B_z = -3$ nT, and $N = 0.7$. In the near-noon sector, the auroral ovals are defined as areas at ionospheric altitude, magnetically connected to a thin equatorial boundary layer adjacent to the subsolar magnetopause. On the nightside, the ovals were assumed to map to a wider equatorial region, corresponding to the innermost part of the tail plasma/current sheet and the outer ring current.

More quantitatively, in the geocentric solar magnetospheric (GSM) equatorial plane the inner and outer boundaries of the 3-D auroral domain were defined as two quasi-circular contours:

$$R_{1,2}(\phi) = R_{S_{1,2}} + (R_{T_{1,2}} - R_{S_{1,2}})\sin^2(\phi/2), \tag{1}$$

passing at $X_{S_{1,2}} = R_{S_{1,2}}$ near the subsolar point at noon and at $X = -R_{T_{1,2}}$ at midnight. Here R and ϕ are the equatorial radial distance and GSM longitude, R_S and R_T are noon and midnight radii of the contours, and the subscripts 1 and 2 denote the inner and outer contours, respectively. To represent an average auroral oval, the following model values (in Earth's radii) were adopted: $R_{S_1} = 10.0$, $R_{S_2} = 10.5$, $R_{T_1} = 6.0$, and $R_{T_2} = 12.0$.

Figure 1 shows in the left panel each contour as 72 white dots, plotted in 5° intervals of GSM longitude against the color-coded background of the total equatorial magnetic field magnitude B. In the right panel, the

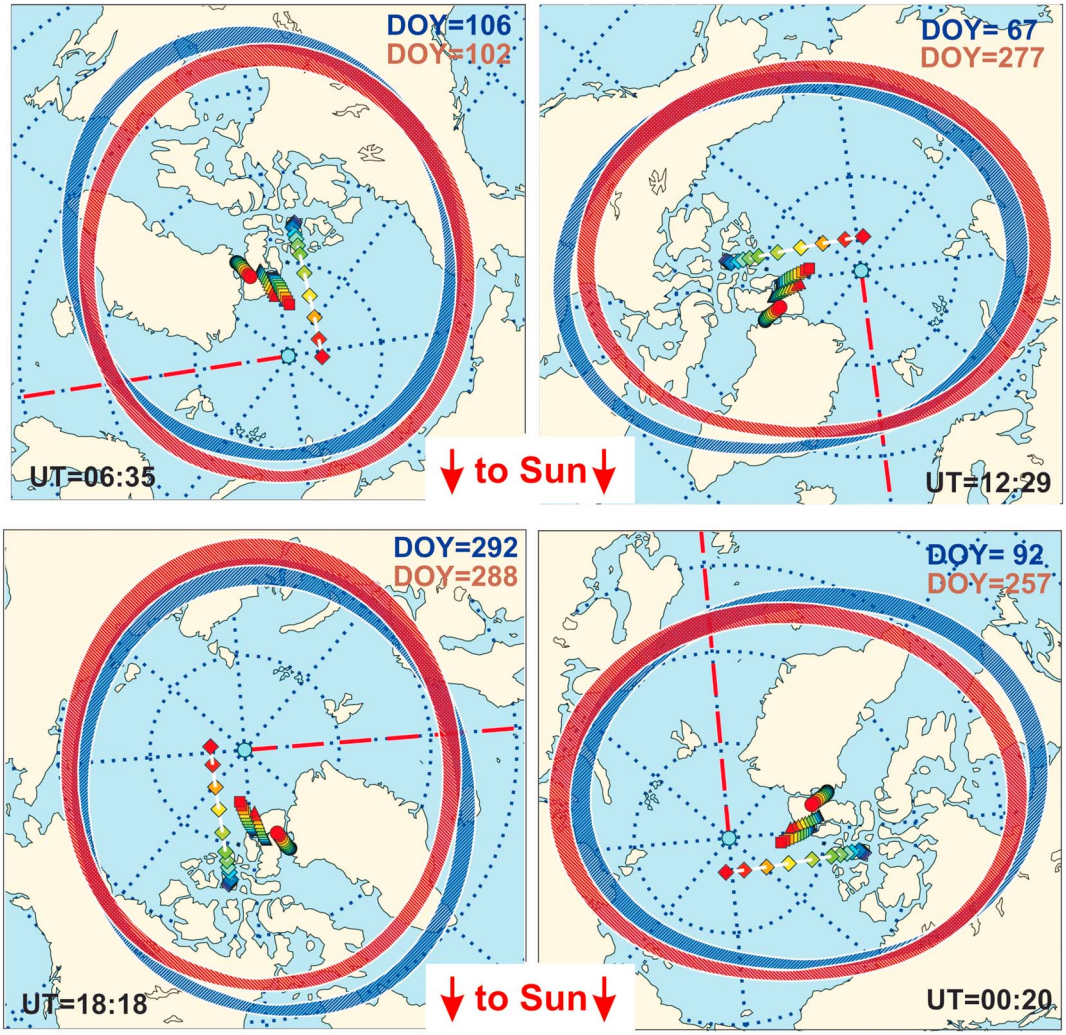

Figure 2. Northern polar plots of the model auroral oval for four universal time (UT) moments and days of year (indicated on each panel) with zero geodipole tilt angle. Blue- and red-shaded ovals correspond to their 1965 and 2020 positions, respectively; the days of year (DOY) are also indicated by fonts of the corresponding color. Geographic North Pole and Greenwich meridian are indicated with small blue circles and red dashed lines, respectively. The colored symbols inside the ovals indicate positions of the centered (circles) and eccentric (squares) dipole axes, corrected geomagnetic pole (triangles), and of the geomagnetic dip pole (diamonds). The sequence of colors from dark blue to yellow to red corresponds to subsequent epochs from 1965 to 2020 at 5-year cadence. The sunward side is at the bottom edge of each panel.

meridional configuration of the model field is displayed, with the auroral oval domain highlighted with dark red. The field lines are plotted in 1° intervals of footpoint latitude λ, starting from the innermost $\lambda = 59°$. At ionospheric altitude, the model auroral ovals span the latitude intervals between ~ ±72° and ~ ±74° at noon and between ~ ±63° and ~ ±67° at midnight. Although quantitative details of such representation may be argued, they are of secondary importance in the context of the present study, focused first of all on the secular shift of the ovals due to the secular evolution of the internal currents, rather than on the distant configuration of the magnetospheric sources of auroras.

The internal component of the total field used in the mapping was represented by the International Geomagnetic Reference Field (IGRF; e.g., Thébault et al., 2015) for 1965 and 2020 epochs. The 2020 coefficients were derived by linear extrapolation of the 2015 model using the available secular velocities. In addition to the spatial secular redistribution of the main field, there was a 3.75% decrease of the Earth's magnetic moment, from $8.00484 \cdot 10^{22}$ A m^2 in 1965 to $7.70476 \cdot 10^{22}$ A m^2 in 2020, which should have resulted (under assumption of the same solar wind pressure) in the magnetopause contraction by ~1.2% and a corresponding

Table 1
Geographic Latitudes (λ) and Longitudes (ϕ) of Ground Crossing Points of the Centered Dipole (CD), Eccentric Dipole (ED), Dip Pole (Dip), and Corrected Geomagnetic Pole (Corr), Calculated for the First and Last Epochs of the Interval 1965–2020 in the Northern (N), and Southern (S) Hemispheres (Degrees)

Epoch	λ_N^{CD}	ϕ_N^{CD}	X^{ED}	Y^{ED}	Z^{ED}	λ_N^{ED}	ϕ_N^{ED}	λ_S^{ED}	ϕ_S^{ED}
1965	78.53	−69.85	−368.8	223.8	133.5	81.40	−86.27	−75.13	119.62
2020	80.59	−73.17	−399.3	370.3	226.6	84.51	−100.00	−75.86	117.01
Epoch	λ_N^{dip}	ϕ_N^{dip}	λ_S^{dip}	ϕ_S^{dip}	λ_N^{corr}	ϕ_N^{corr}	λ_S^{corr}	ϕ_S^{corr}	
1965	75.62	−101.34	−66.33	139.53	80.20	−80.75	−74.10	126.44	
2020	86.39	169.81	−64.11	135.76	83.44	−85.47	−74.35	125.43	

Note. Also listed are geographic Cartesian coordinates $\{X^{ED}, Y^{ED}, Z^{ED}\}$ of the eccentric dipole (kilometers).

~0.6% increase of the auroral oval colatitude. Although quite small, that effect was taken into account by a proper rescaling of the characteristic distances in the external field sources, including the size of the model magnetopause and the mapping parameters entering in (1).

More specifically, under the assumption of constant solar wind pressure P, the force balance implies a simple self-similar relationship (e.g., Siscoe & Chen, 1975) $R_i \propto M_E^{1/3}$ between the geodipole moment M_E and all magnetospheric scale lengths R_i, including the subsolar standoff and terminator radii, the distance to the inner edge of the tail current, and the asymptotic radius of the distant tail. The assumed constancy of P requires the same total intensity of the subsolar magnetic field (hence, the same surface density of the magnetopause current), as well as the same asymptotic value of the tail lobe field (hence, the same density of the distant tail current per unit tailward distance). Such scaling procedure accounts for most of the effect of M_E secular change. In the light of previous studies (Cnossen, 2017, and references therein) the adopted scaling may be viewed as not completely accurate; nevertheless, the main focus of this work is on the secular shift of the ovals, rather than on their expansion/contraction.

To visualize universal time effects due to the Earth's rotation, four UT moments (all with $\Psi = 0$) were selected from different days of year in 1965 and 2020, spaced by roughly 6 hr UT. For each of the four moments, the equatorial dotted contours shown in the left panel of Figure 1 were mapped down to Northern and Southern Hemispheres to the height of ≈140 km, and thus obtained closed loops outlined the inner and outer boundaries of the auroral oval at ionospheric level. The resulting maps of the northern oval are shown in four panels of Figure 2, corresponding to four orientations of the Earth with respect to the Sun.

Several features are immediately apparent in the plots. First, the northern oval is clearly elongated in the direction of the ~100° meridian plane, roughly perpendicular to the Greenwich meridian, in line with the early result of Oguti (1993). In the Earth's frame of reference, both the oval's shape and its shift between 1965 and 2020 are only weakly sensitive to the universal time (under assumption of zero tilt, $\Psi = 0$), except in the near-noon MLT sector associated with the dayside cusp, where the latitudinal shift in the East Canada sector (UT = 18:18, bottom left panel) is distinctly larger than that in the Siberian sector in the eastern hemisphere (UT = 06:35, top left).

Second, the secular shift of the northern oval over the 55-year interval is commensurate with the concurrent shift of the centered dipole (CD) axis crossing point, whose successive locations between 1965 and 2020 are shown in Figure 2 by colored circles, filling the strait between Greenland and Ellesmere Island. The corresponding geocentric (GEO) latitudes and longitudes are obtained from the first three IGRF coefficients as $\lambda_N^{CD} = \arccos\left(-g_1^0/\sqrt{g_1^{0^2} + g_1^{1^2} + h_1^{1^2}}\right)$ and $\phi_N^{CD} = \arctan\left(h_1^1/g_1^1\right)$ (e.g., Akasofu & Chapman, 1972, ch. 2.2.6).

Note that the centered dipole is, in a sense, just a formal abstraction adopted merely out of convenience, to compactly describe the magnetic field in the spherically/axially symmetric geocentric/geodetic coordinate systems. In actuality, the distributed sources of the main field inside the Earth are significantly asymmetric and offset, for which reason their physical "magnetic center" is best represented by an eccentric dipole (ED) rather than by CD. The secular shift of the ED is shown in the plots as a sequence of squares, color coded in the same succession as for the CD. Unlike in the standard ED derivation based on minimization of only second-order coefficients of spherical harmonics (e.g., Langel, 1987, ch. 4, sect. 10.2, and references therein),

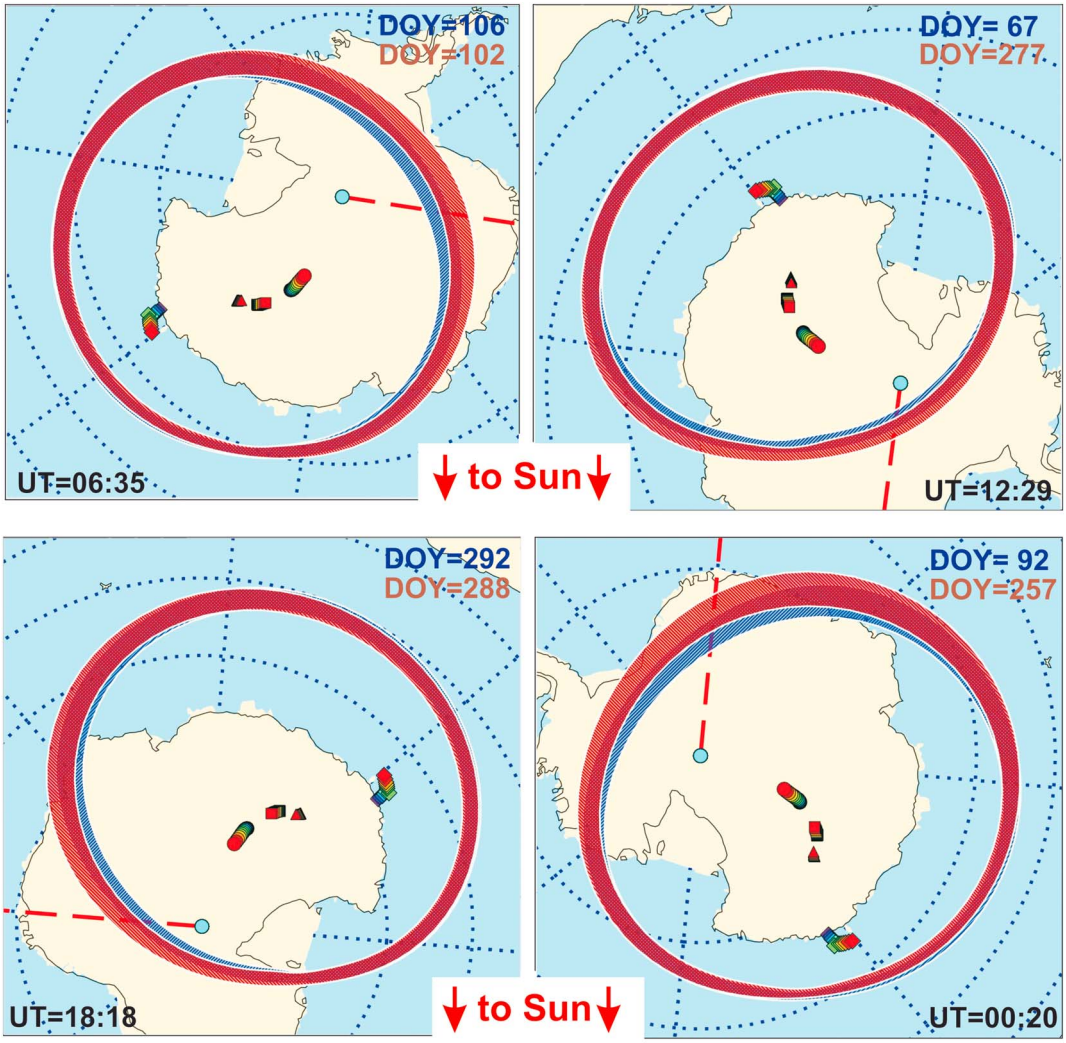

Figure 3. Auroral ovals at the same universal time (UT) moments and in the same format as in Figure 2, but in the southern polar cap. See Figure 2 caption for the notation legend.

in this study the ED coordinates $\{X^{ED}, Y^{ED}, Z^{ED}\}$ were calculated by least squares fitting of the ED field to that given by full IGRF expansion on a geocentric sphere of sufficiently large radius $R = 50\,R_E$ (in order to minimize contributions from all nondipolar harmonics). Values of the above parameters for 1965 and 2020 are given in Table 1.

The next chain of locations marked in Figure 2 by colored triangles illustrates the secular shift of the corrected geomagnetic pole, obtained by tracing an IGRF line (with zero external field) down to Earth from a remote starting point at $Z_{MAG} = 50\,R_E$ on the CD axis, in line with a standard definition of corrected geomagnetic coordinates (Gustafsson, 1970; Hakura, 1965; Hultqvist, 1958). As seen in the plot, the corrected pole locations are quite close to those of ED, and their temporal evolution is also the same. Finally, the colored diamonds mark the dip pole track, calculated by an iterative search in geodetic coordinates of a location with zero horizontal component of the geomagnetic field, based on full IGRF expansions. The plot demonstrates the strikingly fast secular shift of the dip pole, with a notable acceleration by the end of the twentieth century. The dramatic difference with the relatively slow drift of the other poles is largely a local geometrical effect, arising from high sensitivity of the dip pole position to even small variations of the horizontal field component and its low tangential gradient (due to a specific combination of slowly varying higher-order multipoles in the main field expansion).

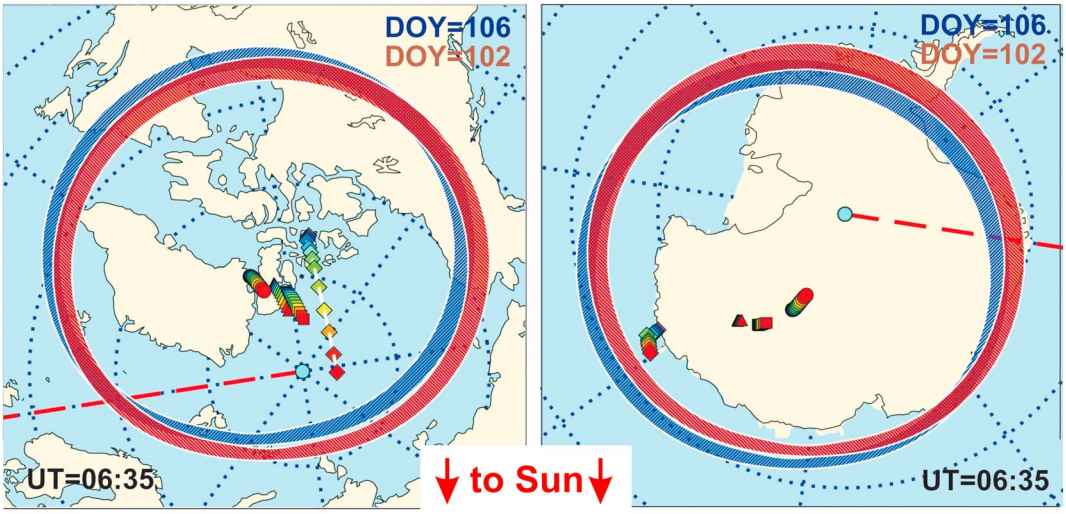

Figure 4. Illustrating the role of higher-order multipoles. Here the northern (left) and southern (right) auroral ovals were obtained using a purely dipolar internal field instead of the full International Geomagnetic Reference Field expansion used to generate the similar plots for UT = 06:35 in Figures 2 and 3. DOY = days of year.

The southern auroral oval was obtained by tracing the model field lines from the same locations in the equatorial plane, but in the opposite directions. The result is shown in Figure 3 in the same format as for the northern polar cap in Figure 2. As can be seen from comparing the plots, the shape of the southern oval is much less elongated and closer to circular than that of the northern oval, which also agrees with the result of Oguti (1993). Overall, the secular shift of the oval between 1965 and 2020 is much less than in the Northern Hemisphere; the largest displacement takes place in the sector roughly centered around the Greenwich meridian.

In regard to the pole behavior, the most striking feature is the dramatically smaller excursion of the southern dip pole: instead of the huge (almost 900 km) jump in the Northern Hemisphere, one sees a relatively small north-west shift by only ~200 km. This interesting asymmetry has been addressed earlier in detail by Mandea and Dormy (2003). The CD pole shift between 1965 and 2020 is (and must be, by definition) equal to that in the Northern Hemisphere; at the same time, the concurrent shifts of the ED and corrected poles are substantially shorter, which is due to the added effect of a significant (by ~180 km) displacement of the ED: by ~93 km northward from the equatorial plane and by ~150 km toward Eastern Siberia. More detailed quantitative data on the pole and ED excursions over the 12 epochs from 1965 to 2020 are given in Table 1.

Finally, an interesting question is the role of nondipolar terms of the IGRF expansion in the obtained auroral oval shapes. Figure 4 shows northern (left) and southern (right) ovals corresponding to UT = 06:35, obtained in the same way as those in the top left plots of Figures 2 and 3, except that all nondipolar coefficients were set equal to zero. Two things are clearly seen: the resulting shapes are much closer to perfect circles and the secular change is now much more uniform, reduced to a simple translation in the direction of the CD/ED pole shift.

Two important comments should be made in the end. First, the present study is limited to only the case of zero dipole tilt, which made it much easier to define the model auroral oval by symmetrically mapping the field lines from the equatorial plane. In strongly tilted configurations, the oval behavior may be somewhat affected by the asymmetry in the insolation of the polar ionosphere and, hence, its conductivity and coupling with the magnetosphere. Second, the assumed simple scaling of the external model field may also be not completely accurate, since it does not take into account changes in the ionospheric conductivity due to the secular variation of the ambient magnetic field. Both the above effects have been discussed in more detail in a recent review by Cnossen (2017); their role in the secular evolution of the auroral ovals will definitely need further study, extending well beyond the scope of the present paper.

3. Summary

Based on an empirical data-based model of the magnetospheric magnetic field in combination with a family of internal IGRF models, the secular evolution of northern and southern auroral ovals has been studied for

the time period between 1965 and 2020. The secular shifts of the ovals were found to be commensurate with the concurrent displacement of the centered, eccentric, and corrected geomagnetic poles, In the Northern Hemisphere, the oval shifted within ∼4° of latitude, approximately in the plane of the ∼100° geographic meridian.

By contrast, the strikingly fast and much larger (by the factor of 4–5) secular shift of the northern dip pole is mostly a geometrical effect due to a weak tangential variation of the horizontal component of the ground geomagnetic field over a relatively wide area along the dip pole track and, as a result, high sensitivity of the dip pole location to even small changes in the internal source distribution. This effect does not result in any abnormalities in the auroral oval behavior. Both the oval shapes and their secular shifts are significantly asymmetric between the Northern and Southern Hemispheres. Thus, in the Southern Hemisphere the oval shifted roughly in the direction of Greenwich meridian and the shift did not exceed 1–1.5° of latitude. The same kind of asymmetry is found in the geomagnetic pole shifts (with exception of the centered dipole).

Acknowledgments
I would like to express my gratitude to Yu. A. Kopytenko for drawing my attention to this problem. Many thanks are due to V. A. Andreeva for her careful reading and penetrating comments on the first version of the manuscript. All Fortran codes used to obtain the above described results are freely available from the author's webpage (http://geo.phys.spbu.ru/~tsyganenko/modeling.html). This work was supported by the Russian Foundation for Basic Research grant 17-05-00415.

References

Akasofu, S.-I., & Chapman, S. (1972). *Solar-terrestrial physics*. Oxford: Clarendon Press.

Cnossen, I. (2017). The impact of century-scale changes in the core magnetic field on external magnetic field contributions. *Space Science Reviews*, *206*, 259–280. https://doi.org/10.1007/s11214-016-0276-0

Gustafsson, G. (1970). A revised corrected geomagnetic coordinate system. *Arkiv för geofysik*, *5*, 595–616.

Hakura, Y. (1965). Tables and maps of geomagnetic coordinates corrected by the higher order spherical harmonic terms. *Report of Ionosphere and Space Research in Japan*, *19*, 121–157.

Hultqvist, B. (1958). The geomagnetic field lines in higher approximation. *Arkiv för geofysik*, *3*, 63–77.

Langel, R. (1987). The main geomagnetic field. In J. A. Jacobs (Ed.), *Geomagnetism* (Vol. 1, pp. 249–512). London: Academic Press.

Laundal, K. M., Cnossen, I., Milan, S. E., Haaland, S. E., Coxon, J., Pedatella, N. M., et al. (2017). North-south asymmetries in Earth's magnetic field: Effects on high-latitude geospace. *Space Science Reviews*, *206*, 225–257. https://doi.org/10.1007/s11214-016-0273-0

Mandea, M., & Dormy, E. (2003). Asymmetric behavior of magnetic dip poles. *Earth Planets Space*, *55*, 153–157.

Newell, P. T., Sotirelis, T., Liou, K., Meng, C.-I., & Rich, F. J. (2007). A nearly universal solar wind-magnetosphere coupling function inferred from 10 magnetospheric state variables. *Journal of Geophysical Research*, *112*, A01206. https://doi.org/10.1029/2006JA012015

Oguti, T. (1993). Prediction of the location and form of the auroral zone: Wandering of the auroral zone out of high latitudes. *Journal of Geophysical Research*, *98*(A7), 11,649–11,655.

Siscoe, G. L., & Chen, C.-K. (1975). The paleomagnetosphere. *Journal of Geophysical Research*, *80*, 4675–4680.

Thébault, E., Finlay, C. C., Beggan, C. D., Alken, P., Aubert, J., Barrois, O., et al. (2015). International geomagnetic reference field: The 12th generation. *Earth Planets Space*, *67*(79), 19. https://doi.org/10.1186/s40623-015-0228-9

Tsyganenko, N. A., & Andreeva, V. A. (2015). A forecasting model of the magnetosphere driven by an optimal solar wind coupling function. *Journal of Geophysical Research: Space Physics*, *120*, 8401–8425. https://doi.org/10.1002/2015JA021641